Modelling and Optimization of CIGS Solar Cell Modules

Joar Johansson

Avdelningen för energi och byggnadsdesign
Institutionen för arkitektur och byggd miljö
Lunds tekniska högskola
Lunds universitet, 2008
Rapport EBD-R--08/19

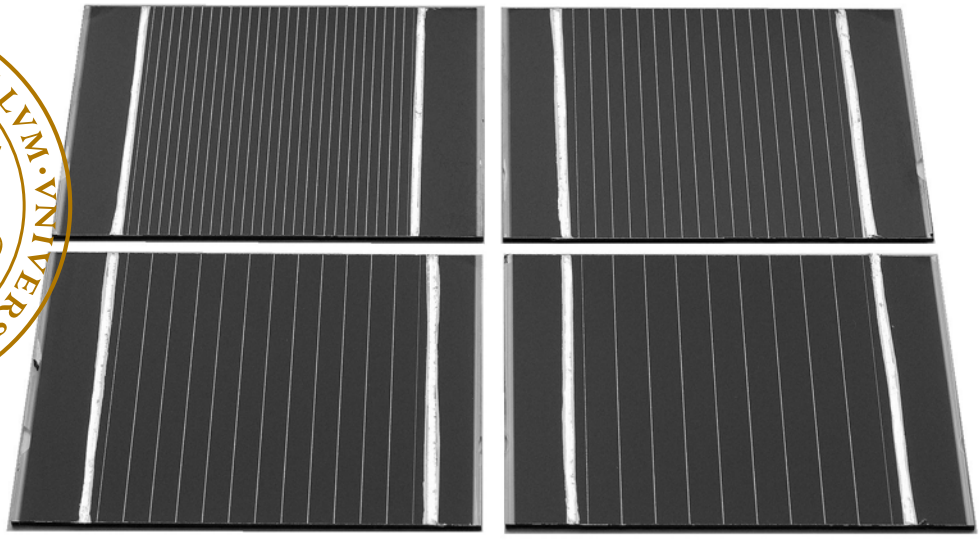

Modelling and Optimization of CIGS Solar Cell Modules

Joar Johansson

Master's Thesis
December 2007

Supervisors: Uwe Zimmermann
Marika Edoff
Examiner: Björn Karlsson

Abstract

The thin-film solar cell module based on $Cu(In, Ga)Se_2$ (CIGS) is a technology with great potential. Two reasons for this are low material consumption and a relatively high efficiency. Low-concentrating systems, which use a large reflector to focus light onto a small area of solar cells, are another technology with potential. Research on both these solar energy technologies is carried out at universities and companies in Sweden.

In this work a computer model of a CIGS solar cell module is built and simulations are performed to optimize the design, i.e. to find the optimal relation between the width of the cells and the sheet resistance of the transparent front contact, at both standard and higher irradiances. The numerical model is based on the one-diode model and takes into account electrical, optical and geometrical parameters. The model is implemented in COMSOL Multiphysics^{TM}, which solves the problem using the finite element method. The optimization is performed in MATLAB®.

Parameters and equations are adjusted to fit measured data and the model is verified by data from manufactured CIGS solar cell mini-modules with different cell widths. The accuracy of the model is shown to be within $\pm 3\,\%$ for the output parameters open-circuit voltage, short-circuit current, fill factor and efficiency. The results from simulations show that a module optimized for an irradiance of $1000\,W/m^2$ has the highest efficiency for a cell width of 3 mm and a front contact sheet resistance of $20\,\Omega/\square$. A module optimized for low concentration, in this case an irradiance of $8000\,W/m^2$, has a cell width of 2 mm and a front contact sheet resistance of $10\,\Omega/\square$.

Contents

1 Introduction **5**

2 Theory **7**
2.1 CIGS Solar Cell Modules 7
2.2 Solar Cell Output Parameters 8
2.3 Diode Equation 9
2.3.1 Diode Saturation Current 9
2.3.2 Current Density 10
2.4 One-Diode Model 10
2.5 Series and Shunt Resistances 11
2.5.1 Resistivity and Conductivity 11
2.5.2 Sheet Resistance 11
2.5.3 Contact Resistance 12
2.6 Transmittance 12

3 Modelling **13**
3.1 CIGS Absorber 13
3.2 Transparent Front Contact 14
3.2.1 Light Transmission 14
3.3 Back Contact 15
3.4 Interconnect Structure 15
3.5 Model Implementation 17

4 Simulations, Results and Discussions **21**
4.1 Parameters Adjustment 21
4.2 Experimental Verification 23
4.3 Cell Width Optimization 24
4.4 ZnO:Al Sheet Resistance Optimization 26
4.5 Irradiance Optimization 27

5 Conclusions **29**

Acknowledgements **31**

References **33**

1 Introduction

A solar cell converts radiant energy into electrical energy. This conversion, which occurs in some semiconductors, is called the photovoltaic effect and was first observed in 1839 by Becquerel. Solar cells manufactured from wafers of crystalline or polycrystalline silicon are today the dominant technology in the commercial market. Solar cells based on a thin film of the semiconductor are another technology with great potential. One such thin-film technology is based on a compound of the elements copper, indium, gallium and selenium, abbreviated $Cu(In, Ga)Se_2$ or CIGS. Two advantages of this thin-film technology are the low material consumption and the high efficiency that has been demonstrated, which both make it economically competitive. Research on CIGS thin-film solar cells is carried out at both Uppsala University and at the company Solibro Research AB.

Low-concentrating systems, which use a large reflector to focus light onto a small area of solar cells, are another technology with potential. The idea is to replace solar cells with cheaper light concentrating devices. Research on such systems is carried out at both the Faculty of Engineering at Lund University and at the company Arontis Solar Concentrator AB.

This study will combine these two research areas. The purpose is to build a numerical model of the CIGS solar cell module which takes into account electrical, optical and geometrical parameters. The model is then used for optimizing the design of the module at different light intensities.

First a model of the CIGS solar cell module is derived. The model, which is based on the one-diode model, is implemented in COMSOL Multiphysics™ and the optimization script is implemented in MATLAB®. Some parameters and equations in the model are adjusted to fit measured data and the model is verified by using data from manufactured CIGS solar cell mini-modules, shown in Figure 1. Finally, simulations are performed to optimize the performance of the CIGS solar cell module with respect to efficiency.

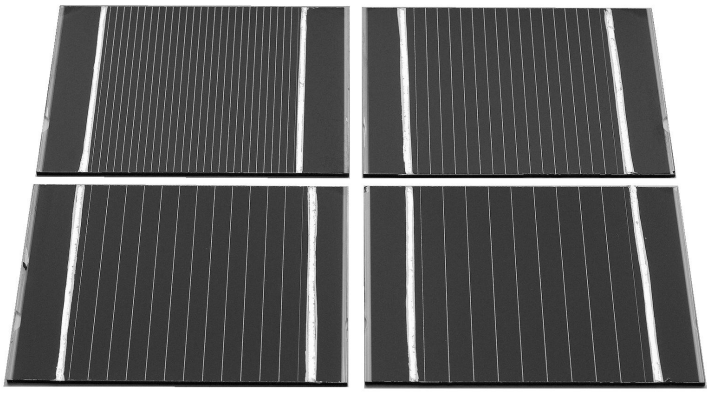

Figure 1. CIGS solar cell mini-modules, with an aperture area of $80\,cm^2$ and cell widths of 3 mm, 5 mm, 7 mm and 9 mm, manufactured at Uppsala University.

2 Theory

2.1 CIGS Solar Cell Modules

A CIGS solar cell is built up of a substrate of soda-lime glass, a back contact of molybdenum (Mo), a light absorbing layer consisting of copper indium gallium diselenide ($Cu(In, Ga)Se_2$), a buffer layer of cadmium sulphide (CdS) or zinc oxy sulphide ($Zn(O, S)$), a thin layer of high resistive zinc oxide (ZnO) and a transparent front contact of aluminium doped zinc oxide (ZnO:Al). Figure 2 shows the cross section of a CIGS solar cell with typical thicknesses of the different layers indicated.

Figure 2. Transmission electron micrograph of the layers in a CIGS solar cell.

In a CIGS solar cell module several cells are connected in series. The series connection is made in an interconnect structure consisting of the three scribes called P1, P2 and P3. Figure 3 shows a series connection of two cells with the cell width, the active cell width, the interconnect structure, the three scribes and the different layers indicated.

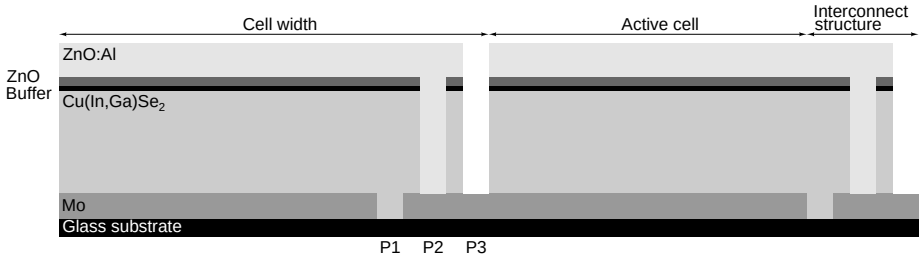

Figure 3. Series connection of two CIGS solar cells. The cell width, the active cell width, the interconnect structure, the three scribes (P1, P2 and P3) and the different layers are indicated. The sketch is not to scale.

CIGS solar cell modules are produced by the research team at Uppsala University and the process involves several different steps. First the Mo is sputtered onto the soda-lime glass. The Mo layer is patterned using a laser and in this way P1 is created. The $Cu(In, Ga)Se_2$ layer is deposited using co-evaporation.

If CdS is used it is prepared by chemical bath deposition (CBD), but if instead the cadmium-free Zn(O, S) is used, it is deposited by atomic layer deposition (ALD). The ZnO layer is sputtered, and then the layers are mechanically scribed and P2 is created. The ZnO:Al layer is sputtered from a ceramic target. The isolation scribe P3 is then created mechanically. The final steps include attachment of electrical wires and encapsulation of the solar cell module using a cover glass, usually with EVA as the laminate material.

2.2 Solar Cell Output Parameters

I–V measurements are performed to characterize solar cells. Figure 4 shows a typical I–V curve with some of the following solar cell output parameters indicated [2]:

- Short-circuit current, I_{sc}, is the maximum current at zero voltage. The short-circuit current density, J_{sc}, is often used (see Section 2.3.2).
- Open-circuit voltage, V_{oc}, is the maximum voltage at zero current.
- Maximum power point, P_{mp}, is the maximum power output at optimal operating condition, i.e. $P_{mp} = V_{mp}I_{mp}$.
- Fill factor, FF, is a measure of how square the I–V curve is. It is defined as
$$FF = \frac{V_{mp}I_{mp}}{V_{oc}I_{sc}} = \frac{P_{mp}}{V_{oc}I_{sc}} \tag{1}$$
- Efficiency, η, is the energy-conversion efficiency. It is given by [1]
$$\eta = \frac{P_{mp}}{P_{in}} = \frac{V_{oc}I_{sc}FF}{P_{in}} \tag{2}$$
where P_{in} is the total power of the incident light.
- Peak power or peak watts, W_p, is the power output at the maximum power point under standard test conditions (STC), i.e. $W_p = P_{mp}$ at STC. The I–V measurement is often performed under STC, which requires an irradiance of $1000\,\mathrm{W/m^2}$, a temperature of $25\,^\circ\mathrm{C}$ and the standard global AM 1.5 spectrum. Modules are usually rated in terms of peak watts.

QE measurements are another method for characterization of solar cells:

- Quantum efficiency, QE, is the number of generated electron-hole pairs per incident photon in the solar cell. When measured with an external circuit this quantity is also referred to as the external quantum efficiency, EQE. It is often measured for wavelengths, λ, in the range from 300 nm to 1300 nm. The short-circuit current density can be calculated from the measurement as
$$J_{sc} = \int_0^\infty \mathrm{EQE}(\lambda)\,\Phi(\lambda)\,d\lambda \tag{3}$$
where Φ is the photon flux at the AM 1.5 spectrum.

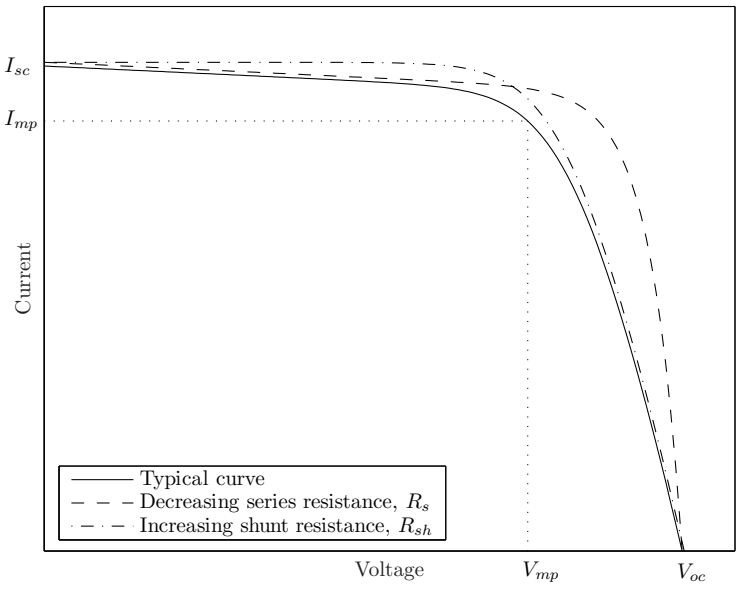

Figure 4. Typical I–V curve showing short-circuit current, I_{sc}, open-circuit voltage, V_{oc}, and the maximum power point, V_{mp} and I_{mp}. The effects of decreasing series resistance, R_s, and increasing shunt resistance, R_{sh}, are also shown.

2.3 Diode Equation

A CIGS solar cell is essentially a heterojunction diode. A heterojunction is formed by joining two different semiconductor materials, such as p-type CIGS and n-type buffer/ZnO. The current through a diode, I_D, is generally described by the diode equation [2]

$$I_D = I_0(e^{qV/AkT} - 1) \tag{4}$$

where V is the applied voltage, I_0 is the diode saturation current (see Section 2.3.1), q is the elementary charge, A is the ideality factor, k is the Boltzmann constant and T is the temperature. For an illuminated solar cell the diode equation becomes [2]

$$I = I_D - I_L = I_0(e^{qV/AkT} - 1) - I_L \tag{5}$$

where I_L is the light-generated current. By definition the I–V curve is often plotted in the first quadrant, and represented by [2]

$$I = I_L - I_0(e^{qV/AkT} - 1) \tag{6}$$

2.3.1 Diode Saturation Current

The diode saturation current, I_0, for a CIGS solar cell is given by [3]

$$I_0 = I_{00}e^{-\Phi_b/AkT} \tag{7}$$

where I_{00} is a prefactor, Φ_b is the barrier height and A is the ideality factor. These quantities depend on the details of each recombination mechanism [4]. It is possible to have recombination in the bulk absorber, in the space charge region of the $Cu(In, Ga)Se_2$ or at the $Cu(In, Ga)Se_2$/buffer interface [3, 4].

If the barrier height is equal to the band gap of $Cu(In, Ga)Se_2$, i.e. $\Phi_b = E_g$, this implies [3]

$$I_0 = I_{00} e^{-E_g/AkT} \tag{8}$$

2.3.2 Current Density

Current density, J, is defined as electric current per cross-sectional area and the unit is A/m^2, but normally the unit mA/cm^2 is used. The diode equation can be expressed using the current density

$$J = J_0(e^{qV/AkT} - 1) - J_L \tag{9}$$

with

$$J_0 = J_{00} e^{-E_g/AkT} \tag{10}$$

Note that the unit for the Boltzmann constant is J/K for Eq. 9 and eV/K for Eq. 10.

2.4 One-Diode Model

A solar cell can be modelled as an electric circuit in the so-called one-diode model. The one-diode model consists of a current generator in parallel with a diode and a shunt resistance, R_{sh}, which are all connected in series with a series resistance, R_s. The equivalent circuit is shown in Figure 5. An equation for the one-diode model is derived using the equivalent circuit and the diode equation.

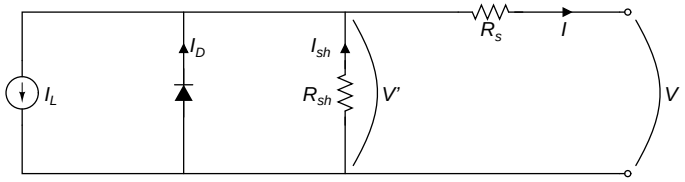

Figure 5. Equivalent circuit of a solar cell according to the one-diode model.

Following Kirchhoff's current law

$$I = I_D + I_{sh} - I_L \tag{11}$$

Kirchhoff's voltage law and Ohm's law give

$$V' = V - IR_s \tag{12}$$

The diode equation (Eq. 4) and Eq. 12 give

$$I_D = I_0(e^{qV'/AkT} - 1) = I_0(e^{q(V-IR_s)/AkT} - 1) \tag{13}$$

Ohm's law and Eq. 12

$$I_{sh} = \frac{V'}{R_{sh}} = \frac{V - IR_s}{R_{sh}} \tag{14}$$

Finally, Eq. 13 and Eq. 14 in Eq. 11 give an equation for the one-diode model [2]

$$I = I_0(e^{q(V-IR_s)/AkT} - 1) + \frac{V - IR_s}{R_{sh}} - I_L \tag{15}$$

2.5 Series and Shunt Resistances

The series resistance, R_s, in a CIGS module is caused for example by the bulk resistance of the semiconductor material [2], the resistance of the transparent front contact and the contact resistance between the front and back contact [6]. The effect of series resistance is shown in Figure 4. The slope of the curve at the open-circuit voltage, V_{oc}, changes as the series resistance changes.

The shunt resistance, R_{sh}, in a CIGS module is caused by for example partial shorting of cells near edges [2] and connection between two adjacent cells through the CIGS in the P1 scribe [6]. The effect of shunt resistance is shown in Figure 4, and it is clear that the shunt resistance changes the slope of the curve at the short-circuit current, I_{sc}.

2.5.1 Resistivity and Conductivity

The electrical resistance, R, of a material is given by

$$R = \rho\frac{l}{A} \tag{16}$$

where ρ is the electrical resistivity, A is the cross-sectional area and l is the length. The unit of resistance is Ω which implies that the unit of resistivity is Ωm. The electrical conductivity, σ, of a material is the reciprocal of electrical resistivity

$$\sigma = \frac{1}{\rho} \tag{17}$$

The unit of conductivity is S/m.

2.5.2 Sheet Resistance

Sheet resistance, $R_\square$, is a measure of electrical resistance of thin films that have a uniform thickness, d, and is defined as [2]

$$R_\square = \frac{\rho}{d} = \frac{1}{d\sigma} \tag{18}$$

Sheet resistance is normally expressed as $\Omega/\square$. Sheet resistance is measured experimentally using a four-point probe and the thickness can be measured using a profilometer.

2.5.3 Contact Resistance

Contact resistance, R_c, is a measure of electrical resistance between two contacting surfaces and is given by

$$R_c = RA_c \tag{19}$$

where R is the resistance and A_c is the area of contact. The unit of contact resistance is normally Ωcm^2.

2.6 Transmittance

The transmittance is the fraction of incident light at a specified wavelength that passes through a sample

$$T(\lambda) = \frac{I_{out}}{I_{in}} \tag{20}$$

where I_{in} is the intensity of the incident light and I_{out} is the intensity of the light coming out of the sample. The transmittance can also be expressed using the exponential Beer-Lambert law

$$T(\lambda) = e^{-\alpha(\lambda)d} \tag{21}$$

where $\alpha(\lambda)$ is the attenuation coefficient and d is the path length.

3 Modelling

The model of a CIGS solar cell module has to take into account electrical, optical and geometrical parameters [6]. Light is absorbed in the solar cell and a current is generated following the diode equation. There is an absorption of light in the transparent front contact which leads to optical losses. Major electrical series and shunt resistances of a CIGS solar cell module are indicated in Figure 6. The lateral current in the transparent front contact (ZnO:Al) and the back contact (Mo) is not uniform, and hence these layers constitute distributed series resistances. The distributed series resistances are $R_{\mathrm{ZnO:Al},1}, R_{\mathrm{ZnO:Al},2}, \cdots, R_{\mathrm{ZnO:Al},n}$ for the ZnO:Al and $R_{\mathrm{Mo},1}, R_{\mathrm{Mo},2}, \cdots, R_{\mathrm{Mo},n}$ for the Mo, as indicated in Figure 6. At the interconnect structure the ZnO:Al carries the full current and is modelled as a discrete series resistance, R_d. There is an additional resistance, R_c, at the ZnO:Al/Mo contact. The CIGS layer provides a shunting path between the front contact and the back contact, indicated by $R_{sh,1}, R_{sh,2}, \cdots, R_{sh,n}$ in Figure 6. The interconnect structure leads to losses in active area. Altogether this leads to a set of nonlinear partial differential equations (PDEs) which can be solved numerically.

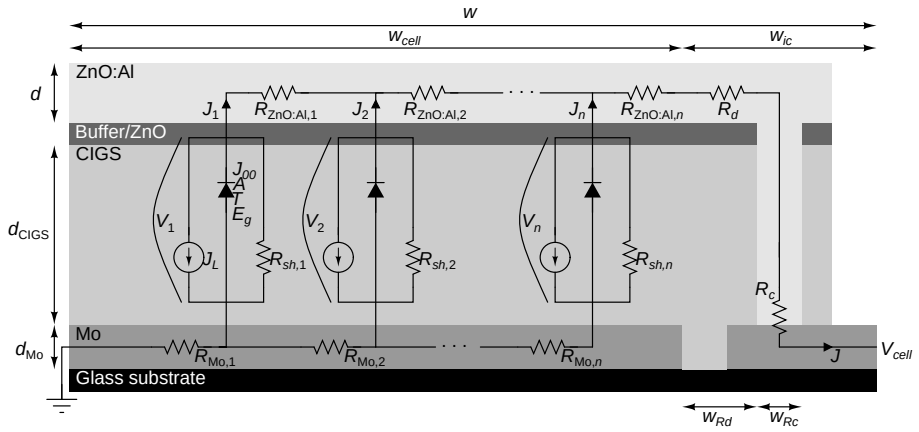

Figure 6. Equivalent electrical circuit of a CIGS solar cell. The one-diode model, shunt resistances and series resistances are shown. Voltages, currents and dimensions are defined. After Ref. [14] and [6].

3.1 CIGS Absorber

A heterojunction is formed at the interface between the p-type $Cu(In, Ga)Se_2$ and the n-type buffer/ZnO layer. The p-type material has a high concentration of holes and a low concentration of electrons, hence holes flow readily through the p-type material [1]. The opposite is true for the n-type material. Excess electron-hole pairs are generated by the light that is absorbed in the CIGS layer. The assymmetrical properties of the heterojunction encourage a flow of generated holes to the back contact and a flow of generated electrons to the n-type material. Therefore, an illuminated heterojunction which is electrically shorted will cause a net current flow. In the model, the current is generated in

each lateral point of the active cell, according to the diode equation (Eq. 9) and Eq. 10 as

$$J_i = J_0 e^{qV_i/AkT} - J_L \tag{22}$$

with

$$J_0 = J_{00} e^{-E_g/AkT} \tag{23}$$

where $i = 1, 2, \cdots, n$ are the lateral points.

The light-generated current, J_L, depends on the transmission of the incident light through the transparent front contact as

$$J_L = T_{\mathrm{ZnO:Al}} J_{L,in} \tag{24}$$

where $T_{\mathrm{ZnO:Al}}$ is a function of the transmittance of the incident light through the ZnO : Al (see Section 3.2.1) and $J_{L,in}$ is the incident light-generated current. The incident light-generated current has a typical value about $350\,\mathrm{A/m^2}$ at STC.

In high-performance CIGS solar cells, the $\mathrm{Cu(In,Ga)Se_2}$ band gap, E_g, is between 1.1 eV and 1.2 eV [3]. The ideality factor, A, depends on the dominant recombination mechanism. It has been demonstrated that the ideality factor is $1 < A < 2$ for CIGS solar cells [3]. The prefactor, J_{00}, has a typical value of about $10^{10}\,\mathrm{A/m^2}$ and the temperature, T, is 298 K at STC. The thickness of the CIGS layer is between $1.5\,\mu$m and $2.0\,\mu$m [5]. In the model, the conductivity of CIGS determines the total shunt resistance, R_{sh}, of the module.

The buffer layer is a prerequisite to form the heterojunction. The thickness of the buffer layer is about $0.05\,\mu$m [5]. The ZnO layer increases the performance of the solar cell. The thickness of the ZnO is about $0.1\,\mu$m [5]. The properties of these layers are included in the modelled CIGS layer.

3.2 Transparent Front Contact

The following relationship holds for the sheet resistance, conductivity and thickness of the ZnO : Al layer (cf. Eq. 18)

$$R_{\square,\mathrm{ZnO:Al}} = \frac{1}{d\sigma_{\mathrm{ZnO:Al}}} \tag{25}$$

Experimental data of the sheet resistance and the thickness of the ZnO : Al layer can be seen in Table 1. In the table the calculated value of the conductivity is also shown. It is clear that the conductivity increases as the thickness increases.

3.2.1 Light Transmission

The optical transmission of the incident light through the transparent front contact decreases sharply when the ZnO : Al layer becomes thicker and as a result has less sheet resistance. A model that describes the transmittance, $T_{\mathrm{ZnO:Al}}$, as a function of the sheet resistance, $R_{\square,\mathrm{ZnO:Al}}$, is [6]

$$T_{\mathrm{ZnO:Al}} = T_1 - \left(\frac{R_1}{R_{\square,\mathrm{ZnO:Al}}}\right)^{m_1} \tag{26}$$

where T_1, R_1 and m_1 are constants adjusted to fit experimental data. For the sake of simplicity the transmission of light is assumed to be independent of the wavelength of the incident light.

Experiments have been performed to determine the transmission through the ZnO:Al layer as a function of its sheet resistance at Solarex Corporation [7], at Uppsala University [8] and in the present study. The fitting parameters are $T_1 = 0.96$, $R_1 = 3.3\,\Omega/\square$ and $m_1 = 3.3$ [6] for the experimental data from Solarex Corporation, and $T_1 = 1$, $R_1 = 0.3707\,\Omega/\square$ and $m_1 = 0.8226$ [8] for the experimental data from Uppsala University. Eq. 26 and the fitting parameters for the experimental data from Solarex Corporation and Uppsala University give the following equations for the transmittance

$$T_{\mathrm{ZnO:Al}} = 0.96 - \left(\frac{3.3}{R_{\square,\mathrm{ZnO:Al}}}\right)^{3.3} \tag{27}$$

$$T_{\mathrm{ZnO:Al}} = 1 - \left(\frac{0.3707}{R_{\square,\mathrm{ZnO:Al}}}\right)^{0.8226} \tag{28}$$

An experiment was carried out to characterize the ZnO:Al from another sputter machine, MRC II, which is used when CIGS mini-modules are manufactured at Uppsala University. Together with monitor samples on plain glass substrates, solar cells with an area of $0.5\,\mathrm{cm}^2$ were prepared with an increasing thickness of the ZnO:Al layer. The short-circuit current density, J_{sc}, for each solar cell was calculated following Eq. 3, see Table 1. The thickness of the ZnO:Al, d, was measured using a profilometer, the sheet resistance of the layer, $R_{\square,\mathrm{ZnO:Al}}$, was measured with a four-point probe and as a result the conductivity of the ZnO:Al, $\sigma_{\mathrm{ZnO:Al}}$, could be calculated, see Table 1. The short-circuit current density decreases as the thickness of the ZnO:Al layer increases due to the higher optical absorption of light in a thicker layer. Using the exponential Beer-Lambert law (Eq. 21) and Eq. 25, a curve, which describes the transmission of the incident light through the ZnO:Al layer, was fitted to the experimental data

$$T_{\mathrm{ZnO:Al}} = e^{-\alpha d} = e^{-\alpha/(R_{\square,\mathrm{ZnO:Al}}\sigma_{\mathrm{ZnO:Al}})} = e^{-1.095/R_{\square,\mathrm{ZnO:Al}}} \tag{29}$$

where the fitting parameters are $\alpha = 1.04\cdot10^5\,\mathrm{m}^{-1}$ and $\sigma_{\mathrm{ZnO:Al}} = 0.95\cdot10^5\,\mathrm{S/m}$.

Figure 7 shows experimental data of $1 - T_{\mathrm{ZnO:Al}}$ as a function of the sheet resistance, $R_{\square,\mathrm{ZnO:Al}}$. The analytical approximations, i.e. Eq. 27, Eq. 28 and Eq. 29, are also shown in the figure.

3.3 Back Contact

The thickness of the Mo layer is typically $0.5\,\mu\mathrm{m}$ and the sheet resistance is about $0.65\,\Omega/\square$ [12]. The conductivity of Mo, σ_{Mo}, can thus be calculated, using Eq. 18, to $3.1 \cdot 10^6\,\mathrm{S/m}$.

3.4 Interconnect Structure

The interconnect structure affects the performance of the solar cell module negatively due to area loss, discrete resistance and contact resistance. The width

Table 1. Experimental data. The short-circuit current density is measured on CIGS solar cells using quantum efficiency measurement. The ZnO:Al sheet resistance and thickness are measured on glass substrates using a four-point probe and a profilometer respectively. The conductivity is calculated.

Sub. no. CIGS	J_{sc} [mA/cm^2]	Sub. no. glass	$R_{\square,\mathrm{ZnO:Al}}$ [$\Omega/\square$]	d [μm]	$\sigma_{\mathrm{ZnO:Al}}$ [S/m]
3074-3838-04	33.6	4141-2	28	0.56	$0.64 \cdot 10^5$
3080-3838-12	31.6	4141-1	11	1.1	$0.83 \cdot 10^5$
3073-3838-05	30.3	4147-2	7.2	1.5	$0.93 \cdot 10^5$
3076-3838-04	29.3	4141-5	5.3	1.9	$0.99 \cdot 10^5$
3078-3838-05	26.9	4142-1	3.4	2.7	$1.1 \cdot 10^5$
3075-3838-12	24.4	4142-2	2.3	3.3	$1.3 \cdot 10^5$

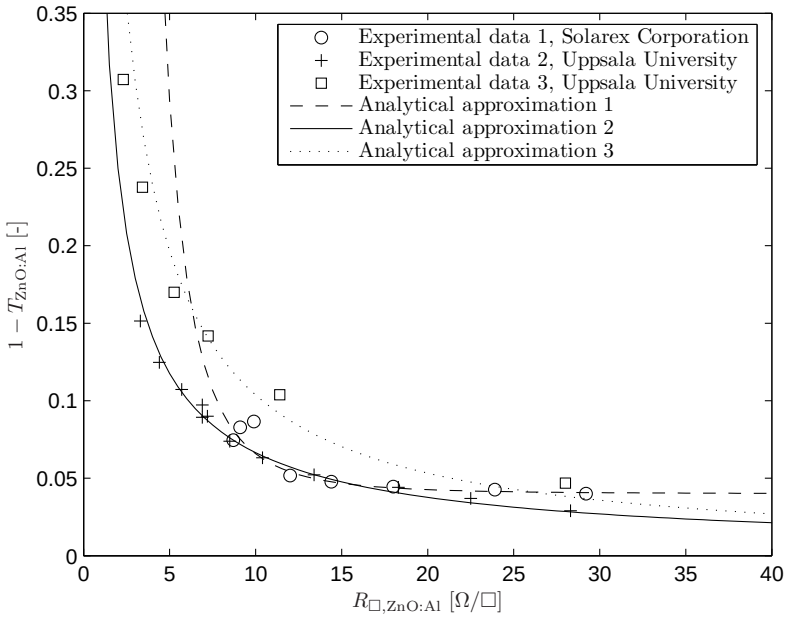

Figure 7. $1 - T_{\mathrm{ZnO:Al}}$ of the ZnO:Al layer as a function of its sheet resistance, $R_{\square,\mathrm{ZnO:Al}}$. Experimental data 1 were taken from Solarex Corporation [7] and data 2 were taken from Uppsala University [8]. Experimental data 3 were produced during the present study. The approximations, i.e. Eq. 27, Eq. 28 and Eq. 29, for each set of experimental data are also shown [6, 8].

of the interconnect structure, w_{ic}, is typically about 300 μm to 400 μm, see Figure 6 [11]. This part of the solar cell is inactive, i.e no current is generated there. The active area loss is simply w_{ic} divided by the cell width, w. In the interconnect structure the full current is carried by the ZnO:Al. The width of this part of the ZnO:Al, w_{Rd}, is typically 160 μm [11]. Both the thickness and the conductivity of this part of the transparent front contact have the same value as the rest of the ZnO:Al.

Contact resistance, R_c, is found at the interconnect between ZnO:Al and Mo. The contact resistance should be lower than 0.01 Ωcm^2 and preferably lower than 0.002 Ωcm^2 according to Ref. [6], and it is about 0.0008 Ωcm^2 according to Ref. [8]. An ongoing study at Uppsala University shows that the contact resistance, which is still a comparatively unknown parameter, is anything from 0.003 Ωcm^2 to very small [13]. The width of the contact, w_{Rc}, is about 50 μm.

3.5 Model Implementation

In broad outline the modelling is done using COMSOL Multiphysics^{TM} and the optimization is performed using MATLAB®. COMSOL Multiphysics (earlier FEMLAB) is a commercial software package for modelling and solving problems based on partial differential equations (PDEs). The PDEs are solved using the finite element method (FEM). FEM is a computer-based general method for numerically solving PDEs. The package contains a number of so-called application modes. An application mode consists of a predefined template and a user interface already set up with equations and variables for a specific area of physics. The software has a graphical user interface but it is also possible to do script programming in the MATLAB language. To do this, the model has to be exported to the MATLAB language as an M-file. Then COMSOL Multiphysics has to be connected to MATLAB, which makes it possible to modify and run the model in MATLAB [9].

The way COMSOL Multiphysics is used in the modelling and solving process is here described in brief. The model is implemented using the Conductive Media DC Application Mode. A 2D geometry model of one single cell and the interconnect structure is created. When the geometry is completed the boundary conditions are set. The electric-potential boundary condition, $V = V_{cell}$, and the ground boundary condition, $V = 0$, specify the voltages at two of the outer boundaries [10]. The electric-insulation boundary condition, $\mathbf{n} \cdot \mathbf{J} = 0$, specifies that no current flows across any of the other outer boundaries. The continuity boundary condition, $\mathbf{n} \cdot (\mathbf{J_1} - \mathbf{J_2}) = 0$, specifies that the normal components of the electric current are continuous across the interior boundary. The conductivity of the materials, constants, and expressions for the generated current, Eq. 22, Eq. 23 and Eq. 24, are all set. An equation that describes the transmission of the incident light, e.g. Eq. 28, is also set.

The software then automatically applies a mesh to the geometry. The mesh-generation process can be controlled through a set of control parameters. A predefined mesh size is chosen. Because of the large difference in dimension between the width and the height of the cell, the geometry has to be scaled before meshing. This geometrical scaling is performed by the software. Next

comes the solution stage for which the software includes a set of numerical solvers. The Nonlinear Parametric solver is chosen and solver parameters are set. COMSOL Multiphysics internally compiles a set of PDEs representing the entire model and solves the problem. The model is solved for the potential, V_{cell}, in the range of 0 V to 0.7 V and each voltage will give an outgoing current density, J. Figure 8 shows the potential distribution of the layers at $V_{cell} = 0.1\,\mathrm{V}$. The model is exported as an M-file.

The optimization script is written in MATLAB. The optimization is carried out by simply varying the cell width, w, and the thickness of the ZnO:Al, d. For each such configuration the model M-file is called and from the solution, which is a J-V curve, it is possible to calculate the solar cell efficiency, η. The optimal design is the one which has the maximum efficiency. Since a CIGS module has a fixed area and a fixed number of cells, the current, I, and the voltage, V, for the module can be calculated. A function is written which calculates other output parameters, such as I_{sc}, V_{oc} and FF.

Scripts and functions have been created with which it is possible to describe the behaviour of a CIGS module. It is also possible to find the optimal relationship between the cell width and the thickness of the ZnO:Al layer. From now on these scripts and functions are just called *the model*. The model has several input parameters. The parameters are summarized in Table 2.

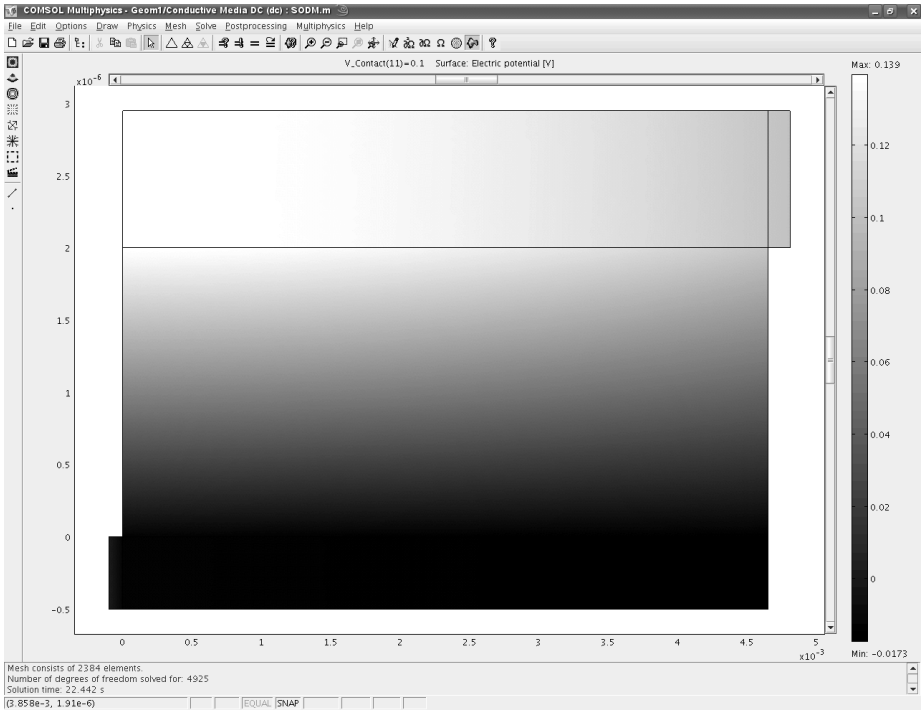

Figure 8. A snapshot of COMSOL Multiphysics showing the potential distribution of the layers in the model at $V_{cell} = 0.1\,\mathrm{V}$.

Table 2. Input parameters for the model. The parameters are **O**ptimized, **G**iven, **M**easured, **A**djusted, an **E**quation or a **C**onstant.

Name	Parameter	Unit	Type
Number of cells	n	-	O or G
Module width	w_{module}	cm	G
Module length	l_{module}	cm	G
Cell width	w	mm	O or G
Active cell width	w_{cell}	mm	O or G
Interconnect width	w_{ic}	μm	M
Interconnect ZnO:Al width	w_{Rd}	μm	M
Thickness ZnO:Al	d	μm	O or M
Thickness CIGS	d_{CIGS}	μm	M
Thickness Mo	d_{Mo}	μm	M
Contact resistance	R_c	$\Omega\mathrm{cm}^2$	A or M
Contact width	w_{Rc}	μm	M
Conductivity ZnO:Al	$\sigma_{\mathrm{ZnO:Al}}$	S/m	A or M
Sheet resistance ZnO:Al	$R_{\square,\mathrm{ZnO:Al}}$	$\Omega/\square$	M
Conductivity CIGS	σ_{CIGS}	S/m	A
Conductivity Mo	σ_{Mo}	S/m	M
Prefactor	J_{00}	$\mathrm{A/m}^2$	A
Band gap	E_g	eV	A or M
Ideality factor	A	-	A or G
Temperature	T	K	G
Irradiance	P_{in}	$\mathrm{W/m}^2$	G
Incident light-generated current	$J_{L,in}$	$\mathrm{A/m}^2$	A
Elementary charge	q	C	C
Boltzmann constant	k	eV/K	C
Diode saturation current	J_0	$\mathrm{A/m}^2$	E
Light-generated current	J_L	$\mathrm{A/m}^2$	E
Transmittance ZnO:Al	$T_{\mathrm{ZnO:Al}}$	-	E, M
Diode equation	J_i	$\mathrm{A/m}^2$	E

4 Simulations, Results and Discussions

4.1 Parameters Adjustment

The parameters in the model are set to fit measured data of an actual mini-module with a cell width of 5 mm and a ZnO:Al sheet resistance of 32 Ω/□. This value of the sheet resistance is too high, and not the optimal one for a cell width of 5 mm. The parameters are set so that the measured I–V curve and simulated I–V curve match each other. Some input parameters are given, some are measured and some have to be adjusted. To get the correct short-circuit current, J_{sc}, the incident light-generated current, $J_{L,in}$, has to be adjusted. The correct open-circuit voltage, V_{oc}, in the model can be achieved by adjusting the prefactor, J_{00}, the band gap, E_g, and/or the ideality factor, A. The ideality factor also has an influence on the shape of the curve.

The series resistance depends on the thickness, d, on the conductivity, $\sigma_{\mathrm{ZnO:Al}}$, of the ZnO:Al layer, and on the contact resistance, R_c. Both the sheet resistance, $R_{\square,\mathrm{ZnO:Al}}$, and the thickness, d, of the ZnO:Al layer are measured, which implies that the conductivity, $\sigma_{\mathrm{ZnO:Al}}$, is also known. So, the contact resistance, R_c, is adjusted to fit the given series resistance. In the same way the conductivity of the CIGS layer, σ_{CIGS}, is adjusted to fit the given shunt resistance. An equation for the transmission of light through the ZnO:Al layer, $T_{\mathrm{ZnO:Al}}$, has also to be chosen. Figure 9 shows the I–V curves of both an actual measured mini-module and a simulated module for which the parameters have been adjusted to correspond to the actual module. The parameters used in the simulation can be seen in Table 3.

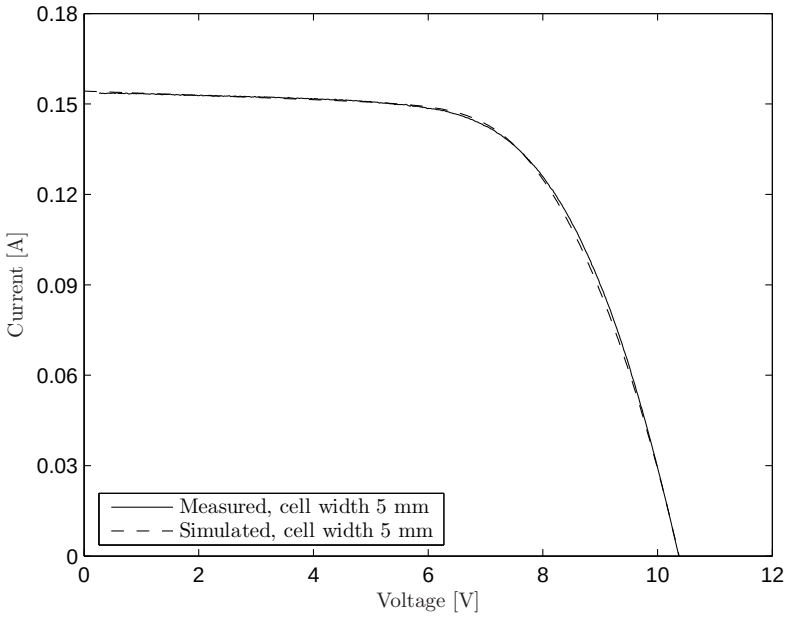

Figure 9. Simulated module with a cell width of 5 mm, which has been adjusted to correspond to an actual module (sub. no. 3709).

Table 3. Input parameters and their values during a specific simulation. Material parameters were adjusted to fit an actual module (sub. no. 3709).

Parameter	Unit	Value
n	-	16
w_{module}	cm	8.00
l_{module}	cm	9.70
w	mm	5.00
w_{cell}	mm	4.70
w_{ic}	μm	300
w_{Rd}	μm	160
d	μm	0.7
d_{CIGS}	μm	2
d_{Mo}	μm	0.5
R_c	$\Omega\mathrm{cm}^2$	0.005
w_{Rc}	μm	50
$\sigma_{\mathrm{ZnO:Al}}$	S/m	$4.5{\cdot}10^{4}$
$R_{\square,\mathrm{ZnO:Al}}$	$\Omega/\square$	31.7
σ_{CIGS}	S/m	$5{\cdot}10^{-5}$
σ_{Mo}	S/m	$3.10{\cdot}10^{6}$
J_{00}	$\mathrm{A/m}^2$	$1.0{\cdot}10^{10}$
E_g	eV	1.2
A	-	1.245
T	K	298
P_{in}	$\mathrm{W/m}^2$	1000
$J_{L,in}$	$\mathrm{A/m}^2$	350
q	C	$1.6{\cdot}10^{-19}$
k	eV/K	$8.62{\cdot}10^{-5}$
J_0	$\mathrm{A/m}^2$	Eq. 23
J_L	$\mathrm{A/m}^2$	Eq. 24
$T_{\mathrm{ZnO:Al}}$	-	Eq. 28
J_i	$\mathrm{A/m}^2$	Eq. 22

4.2 Experimental Verification

Mini-modules with cell widths of 3 mm, 7 mm and 9 mm are simulated and the performances of these modules are compared with measurement data from manufactured modules, see Table 4. This will give an idea of how well the model predicts the performance of modules with different cell widths. All parameters except the number of cells, n, module width, w_{module}, cell width, w, and active cell width, w_{cell}, are kept constant.

Table 5 shows measured and simulated data of mini-modules with cell widths of 3 mm, 7 mm and 9 mm. The corresponding I–V curves can be seen in Figure 10. The conclusion is that the measured and simulated performances of the CIGS solar cell modules agree well. The accuracy of the model is within ±3 % for the output parameters V_{oc}, I_{sc}, FF and η. It should be noted that the low efficiencies at wider cell widths is a consequence of the relatively high sheet resistance of the ZnO:Al layer. The sheet resistance of the manufactured modules was measured at 32 Ω/□.

Table 4. Measured data of CIGS solar cell mini-modules from the same batch but with different cell widths and ZnO:Al sheet resistances. The solar cell output parameters are measured under STC. The sheet resistance is measured using a four-point probe.

Sub. no.	w [mm]	n [-]	$R_{\square,\mathrm{ZnO:Al}}$ [Ω/□]	Area [cm^2]	Area loss [%]	V_{oc}/cell [V]	J_{sc} [mA/cm^2]	FF [%]	η [%]
3810	3	27	32	78.6	10	0.660	30.4	72.2	14.5
3812	3	27	32	78.6	10	0.657	30.3	72.1	14.4
3713†	3	27	32	78.6	10	0.662	31.9	71.4	15.1
3709	5	16	32	77.6	6	0.648	31.7	64.1	13.2
3808	5	16	27	77.6	6	0.648	31.8	64.2	13.2
3809	5	16	27	77.6	6	0.640	31.5	65.4	13.2
3716	5	16	20	77.6	6	0.642	30.5	69.5	13.6
3712	5	16	20	77.6	6	0.645	30.7	68.8	13.6
3813	7	12	32	81.5	4	0.645	32.3	53.9	11.2
3814	7	12	27	81.5	4	0.634	32.3	58.3	11.9
3714	7	12	27	81.5	4	0.638	32.0	60.3	12.3
3711	9	9	32	78.6	3	0.658	33.0	40.6	8.82
3815	9	9	27	78.6	3	0.649	32.7	46.6	9.89
3715	9	9	27	78.6	3	0.640	32.4	47.9	9.93

†This module was prepared with an anti-reflection coating.

Table 5. Measured and simulated output parameters of CIGS solar cell mini-modules with different cell widths. ZnO:Al sheet resistance is equal to 32 Ω/□.

Sub. no.	w [mm]	V_{oc} [V]	I_{sc} [A]	FF [%]	η [%]
3810	3	17.8	0.0885	72.2	14.5
Simulated	3	17.5	0.0890	72.6	14.4
3709	5	10.4	0.154	64.1	13.2
Simulated	5	10.4	0.154	63.9	13.2
3813	7	7.74	0.219	53.9	11.2
Simulated	7	7.78	0.218	52.0	10.9
3711	9	5.92	0.288	40.6	8.82
Simulated	9	5.84	0.281	41.3	8.63

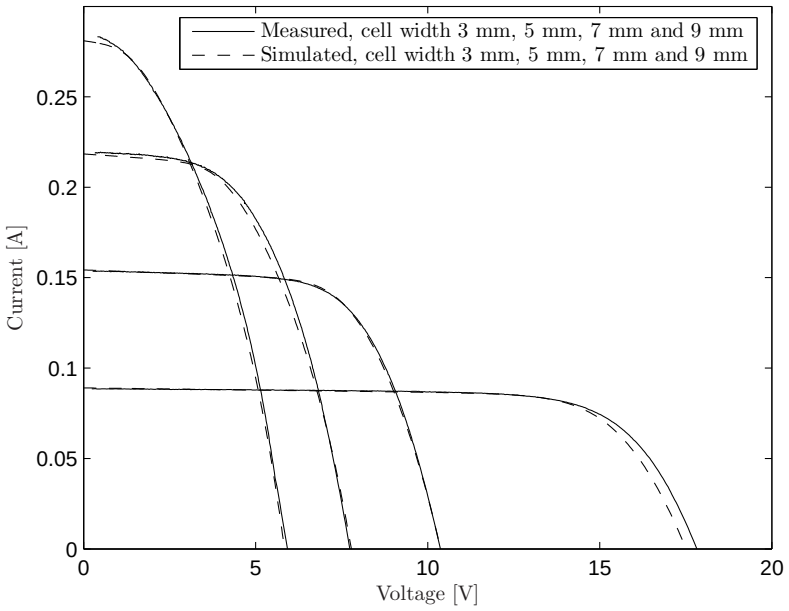

Figure 10. Measured modules (sub. no. 3810, 3709, 3813 and 3711) and simulated modules with cell widths of 3 mm, 5 mm, 7 mm and 9 mm. The material properties were adjusted to match the actual module with a cell width of 5 mm (sub. no. 3709) and then kept constant for the other cell widths.

4.3 Cell Width Optimization

The model is now used to find the optimal cell width, i.e. the cell width which gives the highest module efficiency at STC. The thickness of the ZnO:Al layer, d, is optimized for each investigated cell width. The same values of the parameters are used as in Table 3, except for the conductivity of the ZnO:Al, $\sigma_{\mathrm{ZnO:Al}}$, which is increased from $4.5 \cdot 10^4\,\mathrm{S/m}$ to $1.0 \cdot 10^5\,\mathrm{S/m}$. The higher value of the conductivity is taken from the experimental data in Table 1. For each thickness, d, the corresponding sheet resistance, $R_{\square,\mathrm{ZnO:Al}}$, can be calculated. The number of cells, n, module width, w_{module}, and active cell width, w_{cell}, all vary with the chosen cell width. The simulations are performed for the three equations (Eq. 27, 28 and 29) describing the transmission of light through the ZnO:Al layer, $T_{\mathrm{ZnO:Al}}$.

Figure 11 shows the efficiency, η, of modules with different cell widths. With $T_{\mathrm{ZnO:Al}}$ set equal to Eq. 28 the highest module efficiency, 14.5 %, is found for cell widths between 3 mm and 4 mm. The optimal sheet resistance of the ZnO:Al layer for a cell width of 3 mm is $20.0\,\Omega/\square$, and for a cell width of 4 mm the optimal sheet resistance is $14.5\,\Omega/\square$. A module using a cell width of 5 mm will have a maximum efficiency of 14.3 % with a sheet resistance of $10.5\,\Omega/\square$. In these simulations the interconnect width, w_{ic}, has been set to $300\,\mu$m, which implies an active area loss of 10 % for a cell width of 3 mm and 6 % for a cell width of 5 mm. The higher active area loss for a cell width of 3 mm is more than compensated for by the lower optical losses caused by smaller absorption

of light in the thinner ZnO:Al layer as compared to wider cell widths. For a cell width of 2 mm the active area loss in this case is 15 %, which is too large to be compensated for by the lower optical losses. The highest efficiency for a module with a cell width of 2 mm is 14.1 % with an optimal sheet resistance of 31.1 Ω/□. It is clear that it is more important to decrease the active area losses by minimizing the interconnect width for CIGS modules with narrower cells.

This can be compared with simulations performed in Ref. [5] which gave an optimal cell width of 5 mm at a 10 Ω/□ sheet resistance of the ZnO:Al. $T_{\mathrm{ZnO:Al}}$ for these simulations was also described by Eq. 28. Some other input parameters were not the same, e.g. the maximum efficiency was 12.2 % and the interconnect width was set to 400 μm.

The short-circuit current, I_{sc}, and the open-circuit voltage, V_{oc}, are two other output parameters which change when the cell width of the module is modified, see Table 4. The change of these two output parameters is merely a consequence of the different number of cells.

If $T_{\mathrm{ZnO:Al}}$ is set equal to Eq. 27, the maximum efficiency, 14.6 %, is found for a cell width of 3.5 mm. In this case, the sheet resistance of the ZnO:Al layer is 13.7 Ω/□. For $T_{\mathrm{ZnO:Al}}$ set equal to Eq. 29, the highest efficiency, 14.3 %, is reached using a cell width of 3 mm and a sheet resistance of 24.4 Ω/□. The results of the performed simulations show that any of the three equations describing the transmission of light through the ZnO:Al layer will give about the same optimal cell width.

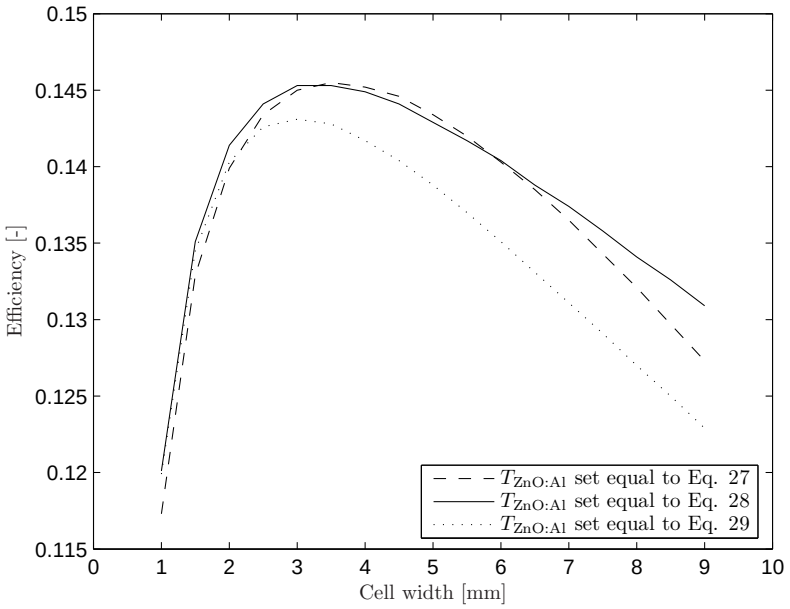

Figure 11. Simulations showing the module efficiency at different cell widths. Three different approximations describing the transmission of light through the ZnO:Al layer are used. The optimal cell width is found between 3.0 mm and 3.5 mm.

4.4 ZnO:Al Sheet Resistance Optimization

Simulations are performed to investigate how the sheet resistance of the ZnO:Al influences the efficiency of the CIGS solar cell module. For each investigated cell width the thickness of the ZnO:Al layer, d, is varied. Since d is varied, the sheet resistance, $R_{\square,\mathrm{ZnO:Al}}$, also changes. The same values of the parameters are used as in Table 3, except for the conductivity of the ZnO:Al, $\sigma_{\mathrm{ZnO:Al}}$, which is set to $1.0{\cdot}10^5$ S/m. The number of cells, n, module width, w_{module}, and active cell width , w_{cell}, all vary with the chosen cell width.

Figure 12 shows the module efficiency, η, at different values of the ZnO:Al sheet resistance, $R_{\square,\mathrm{ZnO:Al}}$. The simulations were performed for modules with cell widths of 3 mm, 5 mm, 7 mm and 9 mm. Measured data from manufactured modules are also plotted in the figure, cf. Table 4. The first conclusion is that the maximum efficiency increases with decreasing cell width for the cell widths investigated. If the shape of the four curves are compared it is clearly seen that the curve becomes flatter around its maximum value with decreasing cell width. So, the narrower cell width the module has, the less sensitive it is to variations of the ZnO:Al sheet resistance, see Table 6. For instance, if the cell width is 3 mm the efficiency is still within 95 % of its maximum value if $R_{\square,\mathrm{ZnO:Al}}$ is in the range 6–60 $\Omega/\square$. For a cell with of 9 mm the corresponding range is 3–11 $\Omega/\square$, which implies a much smaller process window.

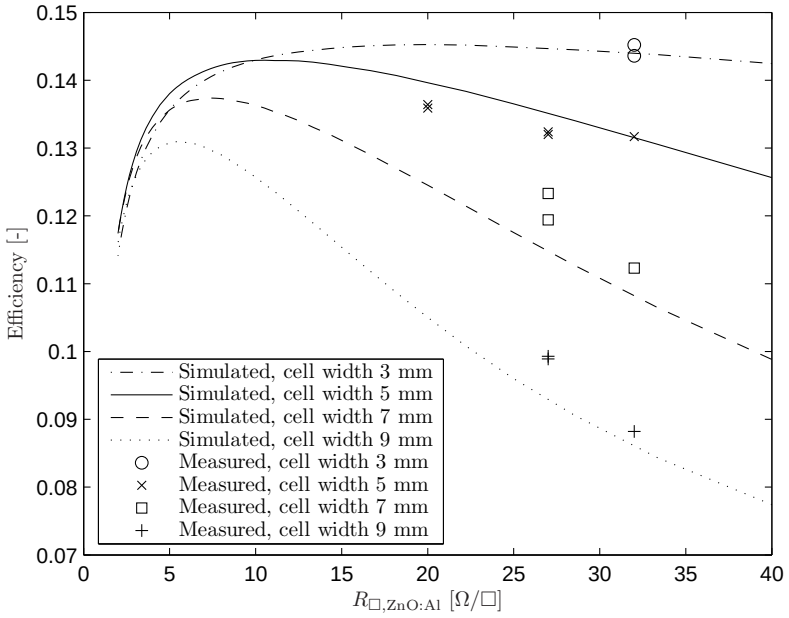

Figure 12. Simulations showing the module efficiency at different values of the ZnO:Al sheet resistance for modules with cell widths of 3 mm, 5 mm, 7 mm and 9 mm. Measured data from Table 4 are also plotted.

It is also interesting to look at the consumption of ZnO:Al during production of CIGS solar cell modules. Modules with cell widths of 3 mm, 5 mm, 7 mm and 9 mm have an optimal $R_{\square,\mathrm{ZnO:Al}}$ of 20.0 $\Omega/\square$, 10.5 $\Omega/\square$, 7.5 $\Omega/\square$, 5.5 $\Omega/\square$

respectively. Since the sheet resistance is inversely proportional to the ZnO:Al thickness, the consumption of ZnO:Al is about twice as high for a cell width of 5 mm, three times higher for a cell width of 7 mm and four times higher for a cell width of 9 mm compared to using a cell width of 3 mm. Except for the smaller material consumption, a thinner layer of ZnO:Al also allows for a faster sputter process. On the other hand, the smaller the cell width of the module the more time it will need in the scribing machine since there are more cells to be scribed. It is clear that other factors than just the efficiency (or peak watts) have to be taken into account when optimizing a CIGS solar cell module for large-scale production.

Table 6. Simulations carried out to optimize the CIGS solar cell modules with respect to efficiency.

w	[mm]	3	5	7	9
$R_{\square,\mathrm{ZnO:Al}}$ at $\eta_{\max}$	[Ω/□]	20.0	10.5	7.5	5.5
$R_{\square,\mathrm{ZnO:Al}}$ at $\eta > 0.95\ \eta_{\max}$	[Ω/□]	6–60	4–25	4–15	3–11
Active area loss	[%]	10	6	4	3
$\eta_{\max}$	[%]	14.5	14.3	13.7	13.1

4.5 Irradiance Optimization

Simulations are carried out to investigate the performance of the CIGS solar cell module at other irradiances than $1000\,\mathrm{W/m^2}$. The optimal relationship between cell width and ZnO:Al sheet resistance is simulated for irradiances of $8\,\mathrm{kW/m^2}$ and $20\,\mathrm{kW/m^2}$. The main parameter varied during these simulations is the irradiance, P_{in}. The incident light-generated current, $J_{L,in}$, will change with the same factor as P_{in}. The parameter $\sigma_{\mathrm{ZnO:Al}}$ is set to $1.0 \cdot 10^5\,\mathrm{S/m}$. The parameters n, w_{module} and w_{cell} all vary with the chosen cell width. The other parameters can be found in Table 3. Note that the temperature, T, is constant at 298 K throughout the simulations.

For an irradiance of $8\,\mathrm{kW/m^2}$ the optimal cell width is 2 mm with a ZnO:Al sheet resistance of $9.9\,\Omega/\square$. This module, optimized for $8\,\mathrm{kW/m^2}$, is called the 8X-module. The so-called 20X-module has an optimal cell width of 1.5 mm with a ZnO:Al sheet resistance of $8.0\,\Omega/\square$. In Figure 13 the efficiency is plotted as a function of the irradiance. The 1X-module with a cell width of 5 mm has its maximal efficiency, 14.3 %, not far from $1\,\mathrm{kW/m^2}$. For the 1X-module with a cell width of 3 mm the maximal value, 14.7 %, is shifted and occurs at about $1.5\,\mathrm{kW/m^2}$. The efficiency decreases fast at higher irradiances for both these modules. The 8X-module has its maximum efficiency, 14.6 %, at $4\,\mathrm{kW/m^2}$, and the 20X-module has its maximum efficiency, 14.0 %, at $7\,\mathrm{kW/m^2}$. The 1X-module has the highest overall efficiency, and it is not possible to reach equally high efficiency for the 8X- and 20X-modules because of the bad transmission of light through the ZnO:Al. The efficiency decreases much more slowly at higher irradiances for both 8X- and 20X-module compared to the 1X-module. This quality makes both the 8X- and 20X-module suitable for low-concentrating systems, such as the Swedish developed systems MaReCo from the company Vattenfall Utveckling AB and Solar8 from the company Arontis Solar Concentrator AB. The results are summarized in Table 7.

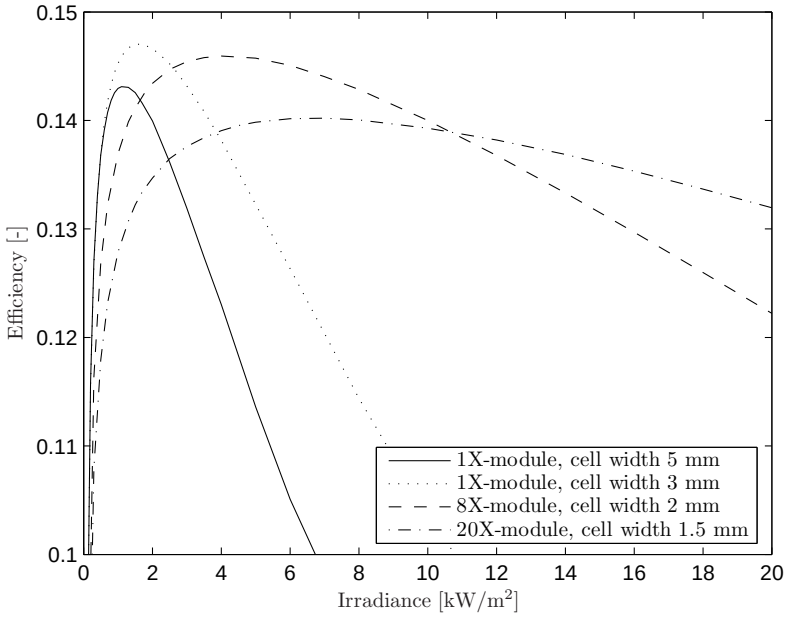

Figure 13. Simulations showing the module efficiency as a function of irradiance for CIGS modules optimized for 1 kW/m^2, 8 kW/m^{2}and 20 kW/m^2.

Table 7. Simulated efficiencies at different irradiances for optimized CIGS modules.

Module	w	$R_{\square,\mathrm{ZnO:Al}}$	η [%] at P_{in} [kW/m^2]				
	[mm]	[Ω/□]	0.5	1	2	8	20
1X	5	10.5	13.7	14.3	14.0	9.13	5.28
1X	3	20.0	13.7	14.5	14.7	11.4	7.09
8X	2	9.90	12.7	13.7	14.3	14.3	12.2
20X	1.5	8.00	11.8	12.8	13.5	14.0	13.2

5 Conclusions

A numerical model of a CIGS solar cell module which is based on the one-diode model and takes into account electrical, optical and geometrical parameters was derived. The model consists of a set of partial differential equations which can successfully be solved using the finite element method. The software package COMSOL Multiphysics, in which the model is implemented, utilizes this method in the solving process. An optimization script was written in the MATLAB language.

A crucial part of the modelling was to describe correctly the optical and electrical behaviour of the transparent front contact. For this reason an experiment was carried out to characterize the ZnO:Al from the MRC II sputter, resulting in an analytical expression. A batch of CIGS mini-modules with an aperture area of 80 cm^2, cell widths of 3 mm, 5 mm, 7 mm and 9 mm and different sheet resistances of the ZnO:Al layer were manufactured.

An efficiency as high as 15.1 % was measured under standard test conditions for one of the modules with a cell width of 3 mm. Another module, with a cell width of 5 mm and a ZnO:Al sheet resistance of 32 $\Omega/\square$, was used as a reference for adjusting parameters in the model. This adjustment was performed by simply varying some of the input parameters in the model until the simulated and measured I–V curves matched each other. An experimental verification of the model was performed by comparing the measured and simulated output parameters of modules with cell widths of 3 mm, 7 mm and 9 mm, all with the same ZnO:Al sheet resistance. The accuracy of the model was shown to be within ± 3 % for the output parameters V_{oc}, I_{sc}, FF and η.

Simulations were performed to optimize the performance of the CIGS solar cell module with respect to efficiency. A module optimized for an irradiance of 1000 $\mathrm{W/m}^2$ has a cell width of 3 mm and a ZnO:Al sheet resistance of 20 $\Omega/\square$. The simulations showed that the higher active area loss for a cell width of 3 mm is more than compensated for by the lower optical losses caused by higher transmission of light through the thinner transparent front contact as compared to wider cell widths. The simulations also showed that the narrower cell width the module has, the less sensitive it is to variations of the ZnO:Al sheet resistance. Simulations were performed to find the optimal design of CIGS modules for low-concentrating systems such as MaReCo and Solar8. One such module, optimized for an irradiance of 8000 $\mathrm{W/m}^2$, has a cell width of 2 mm and a ZnO:Al sheet resistance of 10 $\Omega/\square$.

Acknowledgements

This project, which completes my studies in Engineering Physics, was carried out at Ångström Solar Center, Uppsala University. It was financed by the Swedish SolEl 03-07 programme. First of all I would like to thank my supervisors Uwe Zimmermann and Marika Edoff for their help and guidance. I am particularly grateful to Uwe for fruitful dicussions about the modelling and for help when performing the experiments and manufacturing modules. I would also like to thank the other members of the research team for a pleasant time in their company and for their support, especially Marta Ruth and Per-Oskar Westin for their assistance when manufacturing the modules. I am also indebted to Joakim Byström at Arontis Solar Concentrator AB for suggesting this project to Marika. Finally, I would like to thank Christer and Karen-Marie for the proofreading.

References

[1] M. Green *Solar Cells - Operating Principles, Technology and System Applications*, The University of New South Wales, Kensington, 1992

[2] S. Wenham, M. Green, M. Watt, *Applied Photovoltaics*, The University of New South Wales, Kensington, 2005

[3] W. Shafarman and L. Stolt, $Cu(In, Ga)Se_2$ *Solar Cells*, Handbook of Photovoltaic Science and Engineering, John Wiley & Sons, 2003

[4] U. Rau and H. Schock, $Cu(In, Ga)Se_2$ *Solar Cells*, Clean Electricity from Photovoltaics, Imperial College Press, 2001

[5] J. Wennerberg, *Design and Stability of* $Cu(In, Ga)Se_2$*-Based Solar Cell Modules*, Uppsala, 2002

[6] M. Burgelman and A. Niemegeers, *Calculation of CIS and CdTe module efficiencies*, 1998

[7] S. Wiedeman, J. Kessler, L. Russell, J. Fogleboch, S. Skibo, T. Lommasson, D. Carlson and R. Arya, Proc. 13^{th} European Photovoltaic Solar Energy Conference, Nice, 1995, H.S. Stephens & Associates, 1995, pp. 2059–2062

[8] J. Wennerberg, J. Kessler and L. Stolt, Technical Digest of the International PVSEC-11, Sapporo, Hokkaido, Japan, 1999, pp. 827–828

[9] FEMLAB User's Guide, COMSOL AB, 2004

[10] FEMLAB Modeling Guide, COMSOL AB, 2004

[11] U. Zimmermann, Personal communication, 2007

[12] M. Edoff, Personal communication, 2007

[13] P-O. Westin, Personal communication, 2006

[14] U. Malm, *Stability Characteristics and Modelling of* $Cu(In, Ga)Se_2$ *Solar Cells*, Lecture, Uppsala University, 2006

LUNDS
UNIVERSITET
Lunds Tekniska Högskola

ISSN 1651-8128
ISBN 978-91-85147-27-4